Received: 15 May 2020 | Revised: 26 August 2020 | Accepted: 28 August 2020

DOI: 10.1002/tox.23026

RESEARCH ARTICLE

ENVIRONMENTAL TOXICOLOGY WILEY

Inorganic arsenic-mediated upregulation of AS3MT promotes proliferation of nonsmall cell lung cancer cells by regulating cell cycle genes

Mingjun Sun[1] | Jingwen Tan[2] | Mengjie Wang[2] | Weihua Wen[3] | Yuefeng He[2]

[1]School of Public Health, Dali University, Dali, China

[2]School of Public Health, Kunming Medical University, Kunming, China

[3]Yunnan Center for Disease Control and Prevention, Kunming, China

Correspondence
Weihua Wen, Yunnan Center for Disease Control and Prevention, Kunming, Yunnan 650022, China.
Email: dongsijiehua@sina.com

Yuefeng He, School of Public Health, Kunming Medical University, Kunming 650500, China.
Email: heyuefeng@kmmu.edu.cn

Funding information
National Natural Science Foundation of China, Grant/Award Number: 81160343; Ten Thousand Talent Program of Yunnan Province, Grant/Award Number: YNWR-MY-2018-012; Yunnan Provincial Department of Education, Grant/Award Number: 2019Y0259

Abstract

Long-term arsenic exposure can promote cancer through epigenetic mechanisms, and arsenite methyltransferase (AS3MT) plays an important role in this process. However, the expression patterns and mechanisms of AS3MT in arsenic carcinogenesis remain unclear. In this study, we found that the AS3MT was overexpressed in arsenic exposed population, non-small cell lung cancer (NSCLC) tissues, and A549 cells with sodium arsenite ($NaAsO_2$) treatment for 48 hours. Besides, the level of AS3MT expression was positively correlated with the concentrations of urinary total arsenic (tAs), inorganic arsenic (iAs), methanearsonic acid (MMA), and dimethylarsinic acid (DMA) in all subjects. Functional experiments demonstrated that siRNA-mediated knockdown of AS3MT significantly inhibited proliferation of A549 cells. Mechanism investigation revealed that silencing of AS3MT inhibited proliferation by increasing mRNA expression levels of p21 and E2F1, and inhibiting CDK1, CDK2, CDK4, CDK6, Cyclin A2, Cyclin E1, Cyclin E2, and PCNA mRNA expression. Therefore, arsenic increased AS3MT expression in vivo and in vitro, which could directly act on the cell and affect the progression of NSCLC by regulating cell cycle genes.

KEYWORDS

arsenic, AS3MT, CDKs, cell cycle genes, non-small cell lung cancer, p21, proliferation

1 | INTRODUCTION

Inorganic arsenic (iAs), a toxic metalloid element, has been classified as a human carcinogen by the International Agency for Research on Cancer in 1980. Humans are long-term exposure to arsenic from drinking water and arsenic smelting plants, which poses a major threat to public health.[1,2] Today, about 200 million people in different parts of the world are chronically exposed to potentially toxic levels of arsenic.[3] With the development of industry, agriculture and medicine, occupational exposure to arsenic can occur in a number of work settings including mining and smelting of arsenic-containing minerals, herbicides, and anticancer drugs.[4] In China, lung cancer and skin cancer caused by occupational exposure to arsenic and its compounds have been classified as an occupational disease.

Arsenic was first found to be associated with lung cancer among workers exposed to arsenic.[5] Lung cancer is one of the most lethal malignancies. Approximately 1.6 million people die of lung cancer every year.[6] Epidemiologic studies have showed that squamous cell carcinoma, one of NSCLC, is to be associated with arsenic level in drinking water.[7] Despite progress in treatments for NSCLC, the five-year survival rate was only 16%.[8] Thus, it is necessary to explore underlying mechanism of novel tumor specific growth factor in arsenic carcinogenesis, which will help to develop new strategies for the prevention or treatment of diseases caused by exposure to arsenic.

Accumulating evidence suggests that iAs methylation capability is associated with the rate of malignancy, in particular lung cancer and skin cancer.[9,10] AS3MT plays a key role in the metabolism of arsenic.[11] AS3MT, an enzyme that is encoded by the AS3MT gene in

humans, which catalyzes the transfer of a methyl group from S-adenosy-L-methionine (SAM) to trivalent arsenical.[12] It has been demonstrated that polymorphisms of AS3MT rs11191438 and AS3MT rs1046778 were associated with the risk of bladder cancer and upper tract urothelial carcinoma by affecting arsenic methylation capacity.[13,14] Similarly, AS3MT polymorphisms also impact the risk of lung cancer.[11] Furthermore, AS3MT has been found to be upregulated and negatively correlated with antioncogene mir-548c-3p in arsenic-exposed population.[15,16] Subsequent study found that AS3MT, previously CYT19, was located in the chromosome 10q24.32 as a potential risk factor for the progression schizophrenia.[17] However, Locus 10q24.32 contained typical tumor-related genes, including FGF8 and NPM3.[18] These results indicated that AS3MT is not only involved in arsenic metabolism, but also could be involved in the progression of NSCLC. But, it is unclear whether AS3MT could directly act on the cell and affect the progression of arsenic-induced NSCLC.

Thus, in the study, Our explored the expression of AS3MT in peripheral blood lymphocytes of arsenic plant workers, NSCLC tissues and A549 cells with sodium arsenite ($NaAsO_2$) treatment, and further explored the functions and the potential mechanisms of AS3MT in arsenic-induced NSCLC.

2 | MATERIALS AND METHODS

2.1 | Study subjects and questionnaire interview

In this study, the detailed recruitment protocols of participants were described in the previous study.[19] Briefly, 70 arsenic-exposure laborers were collected from two arsenic plants which were producing arsenic trioxide and 23 individuals in the control group who resided in villages away from the two arsenic plants more than 10 km. Structural questionnaires were performed to collect information from each subject. The information included demographic characteristics, lifestyle factors, and family member history. Five milliliters of fasting venous blood and 20 mL urine samples were derived from subjects in both groups in the morning for subsequent experiments. The study was approved by the ethics committee of Kunming Medical University.

2.2 | Determination of urinary arsenic species levels

The atomic absorption spectrophotometer with an As speciation pretreatment system was used to analyze iAs, methanearsonic acid (MMA) and dimethylarsinic acid (DMA) in urine. Arsenic speciation analysis was based on the well-established hydride generation of volatile arsines, followed by cryogenic separation in liquid nitrogen.[20] The detection limit of this method was 2 ng mg/g creatinine was used to indicate urinary arsenic concentration. The total arsenic (tAs) = iAs + MMA + DMA.

2.3 | Tissue samples

The project was approved by the ethics committee of Kunming Medical University. In obtaining informed consent, all tissue samples were derived from 14 patients who without history of arsenic exposure. In this study, all the samples including NSCLC tissues (n = 14), lymph node tissues (n = 10) and adjacent normal lung tissues (n = 14) (at a distance of >3 cm from the edge of the primary tumor) were obtained from the Third Affiliated Hospital of Kunming Medical University since January to June 2018. All lymph node tissues were reviewed and proved to be metastatic by two independent pathologists. The tissues were immediately immersed in RNAlater stabilization solution (Thermo Scientific) and then shifted to −80°C freezer for storage until been used.

2.4 | Cell culture and treatments

Human NSCLC cell line, A549, was purchased from the Cell Bank of the Chinese Academy of Sciences (Kunming, China). The cell line was cultured in RPMI-1640 medium (HyClone) containing 10% fetal bovine serum and 1% penicillin/streptomycin (Solarbio, Beijing, China). The cells were incubated in an incubator containing 5% CO_2 at 37°C. A549 cells in logarithmic growth phase with a density of 2.5×10^5 cells/well were seeded into a 6-well plate. After 18 hours, $NaAsO_2$ was dissolved in deionized water to generate 2 mM stock solution and added into the culture medium at different concentrations of 0, 20, 40, or 60 μm for 48 hours.

2.5 | RNA isolation and quantitative real-time PCR (qRT-PCR)

The total RNA was extracted from peripheral blood lymphocytes, NSCLC tissues and A549 cell lines using the RNAiso plus reagent (TaKaRa, Beijing, China) and transcribed into cDNA using the HiFiScript cDNA Synthesis Kit (CoWinBiotech, Beijing, China) according to the manufacturer's instructions. The qRT-PCR was performed using the SYBR Green PCR Master Mix (CoWin Biotech, Beijing, China) on a LightCycler 96 instrument Real-Time PCR system (Roche Molecular Systems, California). All primers were synthesized by GenePharma and β-actin was used as an internal reference. The relative expression levels of all genes were described as $2^{-\Delta\Delta Ct}$ and $-\Delta\Delta Ct$ in cell lines and tissues, respectively. The sequences of target genes presented in Table 1.

2.6 | Cell transfection

RFect and siRNAs transfection reagent were purchased from Biogenerating Biotechnologies (Changzhou, China) and GenePharma (Shanghai, China), respectively. A549 cells in logarithmic growth phase with a density of 7×10^4 cells/well were seeded into a 6-well plate. At 19 hours after cultured, 40 nM siRNA duplex and 4 μL RFect

TABLE 1 The sequences of primer used for qRT-PCR

Gene	Sequence
AS3MT	Forward: AGTTATCGGTGACTGTCGTTT
	Reverse: ATGTCCTGTAATTCCTCCATT
CDK1	Forward: TAGCGCGGATCTACCATACC
	Reverse: CATGGCTACCACTTGACCTGT
CDK2	Forward: GAGCTTAACCATCCTAATATTGTC
	Reverse: GCTGGAACAGATAGCTCTTGA
CDK4	Forward: CTGGACACTGAGAGGGCAAT
	Reverse: TGGGAAGGAGAAGGAGAAGC
CDK6	Forward: GTGAACCAGCCCAAGATGAC
	Reverse: TGGAGGAAGATGGAGAGCAC
Cyclin A2	Forward: GGATGGTAGTTTTGAGTCACCAC
	Reverse: CACGAGGATAGCTCTCATACTGT
Cyclin D1	Forward: CAGATCATCCGCAAACACGC
	Reverse: AAGTTGTTGGGGCTCCTCAG
Cyclin D2	Forward: TGATGGGGAAGGAGTACAAA
	Reverse: TTGGAAGAAGAAGCAGGATG
Cyclin E1	Forward: CTTCACAGGGAGACCTTTTAC
	Reverse: CATTCAGCCAGGACACAATAG
Cyclin E2	Forward: GATGGTGCTTGCAGTGAAGAGGA
	Reverse: ACAAGGCAGCAGCAGTCAGTATT
P21	Forward: CAGGGTGCCAGAAGAGTGAG
	Reverse: AGACTAAAGCTCCTACTTCAGCAG
E2F1	Forward: ATGTTTTCCTGTGCCCTGAG
	Reverse: ATCTGTGGTGAGGGATGAGG
PCNA	Forward: GAAGCACCAAACCAGGAGAA
	Reverse: TCACTCCGTCTTTTGCACAG
β-actin	Forward: CCCTGTACGCCAACACAGTGC
	Reverse: ATACTCCTGCTTGCTGATCC

transfection reagent were added to each tube of 100 μL RPMI-1640 medium for incubating 5 minutes at room temperature. After 20 minutes, complex was cultured in a 6-well plate for 24 hours, then 4000 μL of complete medium was replaced. The transfection efficiency was measured by observing with fluorescence microscope and detecting the AS3MT expressions with qRT-PCR at 6 hours and 72 hours after transfection, respectively. The cells were divided into three groups: siCtrl group, siAS3MT # 1 group and siAS3MT # 2 group. The sequences of siRNA presented in Table 2.

2.7 | MTS assay

Cell viability was measured using the CellTiter 96 AQueous One Solution Cell Proliferation Assay system (Promega Biosciences) according to the manufacturer's instructions. For the cells exposed to arsenic, A549 cells were seeded and cultured in 96-well culture plates at a concentration of 1×10^4 cells/well. After 22 hours, $NaAsO_2$ was added into the culture medium at different concentrations of 0, 20, 40 or 60 μm for 48 hours. For the transfected cells, A549 cells were seeded into a 96-well plate at a concentration of 2000 cells/well. After transfection, cells were cultured with 100 μL complete medium for 72 hours. After the treatments, 10 μL of CellTiter 96 AQueous One Solution reagent was added into each well and incubated for 0.5 hour in humidified 5% CO_2 atmosphere. The results were analyzed by the enzyme mark instrument at the absorbance of 490 nm.

TABLE 2 The sequences of siRNAs used for transfection

Gene	Sequence
siCtrl	Forward: UUCUCCGAACGUGUCACGUTT
	Reverse: ACGUGACACGUUCGGAGAATT
siAS3MT # 1	Forward: GCAGCUAUCUUGAAGAAUU
	Reverse: AAUUCUUCAAGAUAGCUGC
siAS3MT # 2	Forward: GGAGAGAAGUUGCCAACAU
	Reverse: AUGUUGGCAACUUCUCUCC

2.8 | Cell proliferation assay

BeyoClick EdU Cell Proliferation Kit with Alexa Fluor 555 (Beyotime, Shanghai, China) was used to detect single proliferating cell. The cells were seeded into a 6-well plate at a density of 7×10^4 cells/well. At 72 hours after transfection, the cells were stained using Azide-555 and Hoechst-33 342 according to the manufacturer's instructions and observed by fluorescence microscope at the maximum emission wavelength of 565 nm and 460 nm, respectively. The cells in the image were counted by the imageJ software and calculated proliferation efficiency.

2.9 | Statistical analysis

All experiments were carried out in triplicate. Data analyses were performed using SAS software package, GraphPad Prism 7.0 and imageJ software. The data were described as the means ± SEM. The Chi-square test was used to assess the efficiency of Cell proliferation between siCtrl groups and siAS3MT groups. The difference between two groups and multiple group comparisons were analyzed by Student's *t*-test and one-way ANOVA, respectively. Pearson correlation coefficient was performed to analyze associations between concentrations of different arsenic species and AS3MT expression. Differences were considered statistically significant at $P < .05$.

3 | RESULTS

3.1 | Characteristics of the subjects and urinary arsenic species

There are no statistical differences in age, smoking and drinking among the exposed laborers in exposed group and control group.

However, compared with control group, the concentration of tAs, iAs, MMA, and DMA was significantly increased in exposed group. General characteristics and urinary three arsenic species of the study subjects were showed in Table 3 and this have been described in our previous articles.[19]

3.2 | AS3MT mRNA expression and its relationship with the concentrations of tAs, iAs, MMA, and DMA in individual subjects

We determined AS3MT mRNA expression in arsenic-exposure group (n = 70) and control group (n = 23) by qRT-PCR. The result indicated that AS3MT mRNA expression in exposure group (4.47 ± 0.26) was significantly increased than that in control group (3.42 ± 0.21) ($P < .05$) (Figure 1A). Pearson correlation analysis indicated that the level of AS3MT expression was positively correlated with the concentrations of urinary tAs, iAs, MMA, and DMA in all subjects. The results were showed in Figure 1B and Table 4.

TABLE 3 General characteristics of subjects and urinary arsenic levels

Variables	Control group (n = 23)	Exposure group (n = 70)
Age	33.84 ± 3.07	36.13 ± 6.02
Smoker (Y/N)	13/10	43/27
Drinker (Y/N)	11/12	35/35
iAs	1.97 (1.18-4.17)	99.52 (49.36-252.36)**
MMA	1.65 (0.83-2.49)	139.98 (56.41-337.54)**
DMA	16.13 (10.56-39.28)	490.60 (174.92-1217.01)**
tAs	19.95 (12.27-32.96)	732.42 (325.59-1726.17)**

Note: iAs, MMA, DMA, tAs were described as (Median, 25-75 percentiles).
**Comparison with the control group, $P < .01$.

3.3 | NaAsO2 induced AS3MT mRNA expression in A549 cells

Epidemiological data showed that arsenic-exposure promoted AS3MT mRNA expression in vivo. After $NaAsO_2$ treatment, the cell viability was evaluated by MTs assay. The result indicated that $NaAsO_2$ significantly inhibited the cell viability (Figure 2A). Next, we detected the AS3MT mRNA expression with $NaAsO_2$ treatment. The data released that the expression ofAS3MT mRNA was significantly increased by $NaAsO_2$ treatment (40, 60 μm) than in control and 20 μm (Figure 2B), implying that sodium arsenite has increased the AS3MT mRNA expression in a concentration-dependent manner in A549 cells.

3.4 | Characteristics of the patients

A total of 14 patients were analyzed, with 10 (71.3%) males and 4 (28.7%) females. The median age of the study subject was 57.8 years (35-75 years), with 8 (57.1%) were smokers and 5 (35.7%) were drinkers.

3.5 | AS3MT was overexpressed in human NSCLC tissues

Epidemiological investigations had indicated that arsenic-exposure promoted AS3MTmRNA expression in subjects. Initially, we evaluated

TABLE 4 Associations of three arsenic species with gene expression in all subjects

	iAs		MMA		DMA	
Variables	*R*	*P*	*R*	*P*	*R*	*P*
AS3MT Expression	0.22	<.05	0.24	<.05	0.25	<.05

Note: Data analyses were performed by Pearson's correlation to urinary iAs, MMA, DMA with gene expression.

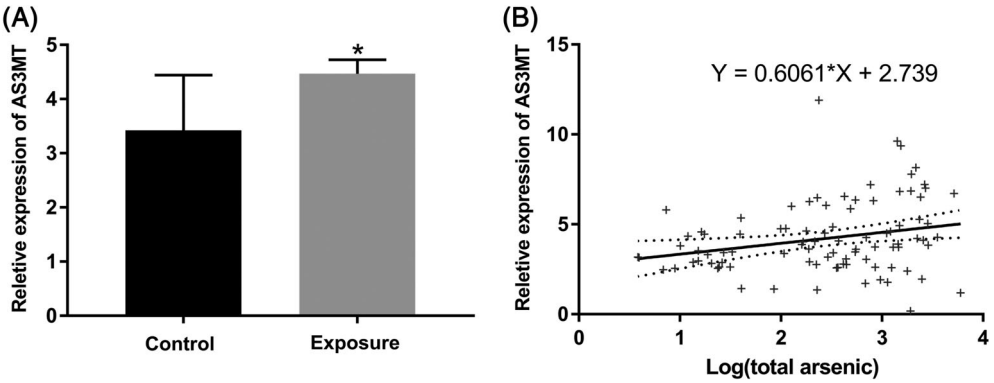

FIGURE 1 AS3MT mRNA expression and its relationship with total arsenic level in arsenic-exposed population. A, AS3MT expression in the exposure group was higher than those in the control group (mean ± SEM, with Student's *t*-test).*$P < .05$. B, AS3MT mRNA expression was positively correlated with the total arsenic in all subjects. The *X*-axis shows the Log(total arsenic) and the *Y*-axis shows the level of AS3MT expression in peripheral blood lymphocytes. Black dots represent a 95% confidence interval ($R^2 = 0.06$, $P < .01$, with Pearson's correlation analysis)

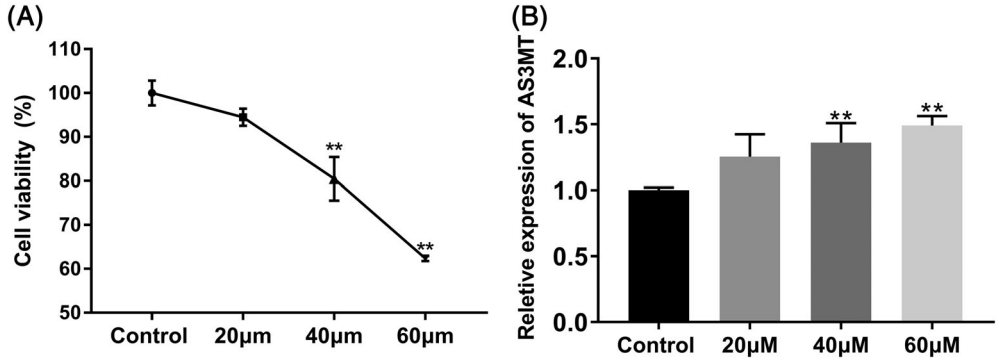

FIGURE 2 $NaAsO_2$ induced AS3MT mRNA expression in A549 cells. After $NaAsO_2$ treatment for 48 hours, A, the results of MTS assay revealed that $NaAsO_2$ inhibited the cell viability in concentration-dependent manner (n = 3). B, AS3MT mRNA expression was increased gradually in a concentration-dependent manner in A549 cells (n = 5) (mean ± SEM, with variance analysis). $^{**}P < .01$

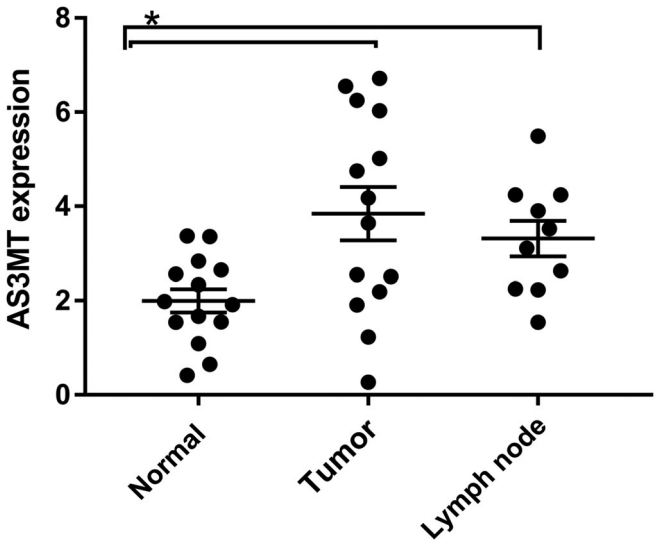

FIGURE 3 Overexpression of AS3MT in NSCLC tissues and lymph node tissues. As showed in the figure, AS3MT mRNA was significantly overexpression in the NSCLC tissues (n = 14) and lymph node tissues (n = 10) compared with the adjacent normal lung tissues (n = 14) (mean ± SEM, with Student's *t*-test). $^{*}P < .05$

AS3MT expression in human adjacent normal lung tissues (n = 14), NSCLC tissues (n = 14) and lymph node tissues (n = 10) by qRT-PCR. The qRT-PCR indicated that the expression of AS3MT mRNA in NSCLC tissues and lymph node tissues were significantly increased than that in adjacent normal lung tissues ($P < .05$). Besides, compared to the NSCLC tissues, the expression of AS3MT mRNA in lymph node tissues had not significantly changed ($P > .05$) (Figure 3).

3.6 | Knockdown of AS3MT was observed in A549 cells

At 6 hours after transfection, AS3MT transfection efficiency was analyzed by fluorescence microscope. The results showed that the transfection efficiency was >80% and the status of the cells were normal (Figure 4A), making these cells suitable for subsequent experiments. Furthermore, at 72 hours after transfection, the qRT-PCR results revealed that the expression of AS3MTmRNA of siAS3MT # 1 groups (0.41 ± 0.02) and siAS3MT # 2 groups (0.57 ± 0.04) were significantly lower than that of siCtrl groups (1.01 ± 0.10) ($P < .05$) (Figure 4B). Thus, above results indicated that the level of expression significantly decreased after AS3MT knockdown.

3.7 | Knockdown of AS3MT significantly inhibited cell viability and proliferation in A549 cells

At 72 hours after transfection, the results of MTS assay showed that knockdown of AS3MT significantly decreased the viability in siAS3MT # 1 groups (49.70% ± 0.72%) and siAS3MT # 2 groups (57.67% ± 0.98%) compared with the siCtrl groups (100.00% ± 1.20%) ($P < .05$) (Figure 5A), which indicates that AS3MT could contributes to proliferation of NSCLC. Furthermore, to assess whether knockdown of AS3MT may cause inhibited proliferation in A549 cells, single proliferating cell assay was conducted to measure cell proliferation of A549 cells upon transfection with siRNAs for 72 hours. We found that the number of single proliferating cells in siAS3MT groups were significantly lower than that in the siCtrl group (Figure 5B). In addition, the quantitative analysis by imageJ software revealed that the number of single proliferating cells account for 52.6%, 24.4%, and 27.5% in siCtrl group, siAS3MT # 1 group and siAS3MT # 2 group, respectively ($P < .05$) (Figure 5C). Overall, our results indicated that knockdown of AS3MT could suppressed the viability and proliferation of A549 cells.

3.8 | Knockdown of AS3MT inhibited expression levels of CDKs, cyclinA2, cyclinD1, cyclinD2, cyclinE1, cyclinE2, PCNA, and induced expression levels of p21, E2F1 in A549 cell lines

To explore the mechanisms underlying AS3MT induced proliferation of lung cancer cells, we found the expression levels of cell cycle genes by

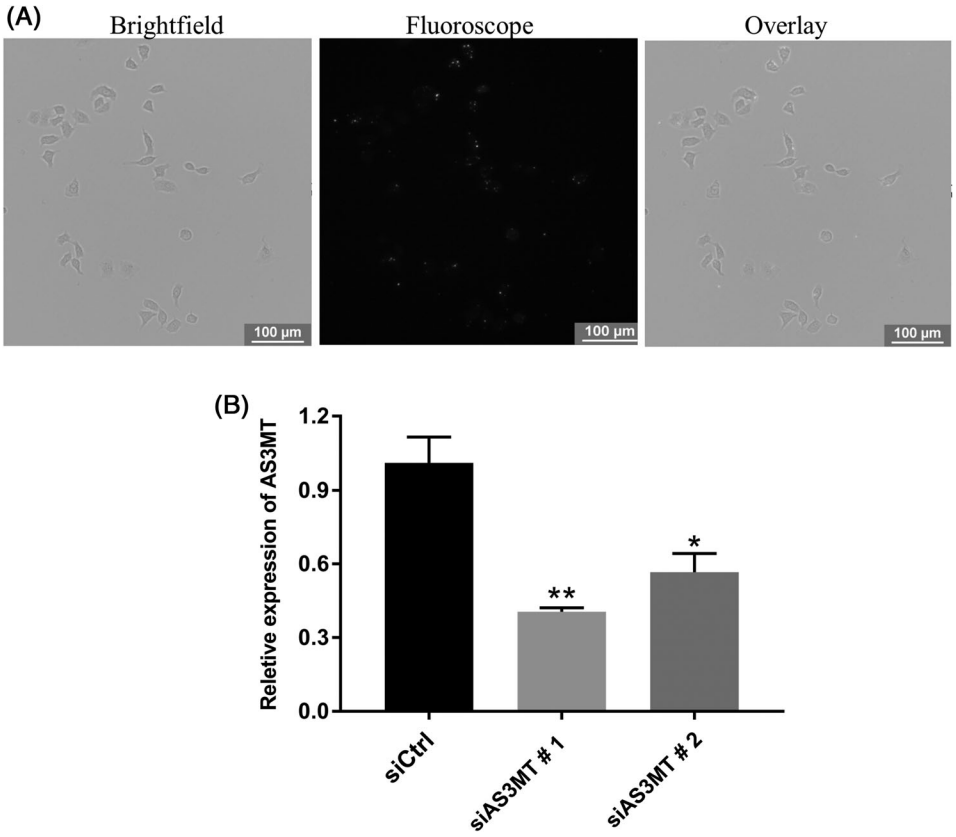

FIGURE 4 SiRNA transfection reagent offered the highest transfection efficiency, and inhibited AS3MT mRNA expression in A549 cell lines. A, At 6 hours after transfection, the transfection efficiency of cells reached >80% and the status of the cells was normal, as assessed by fluorescence microscopy. B, At 72 hours after transfection, relative AS3MT mRNA expression was significantly inhibited in siAS3MT groups compared with the siCtrl groups, as assessed by RT-qPCR (n = 3) (mean ± SEM, with Student's *t*-test). **P* < .05, ***P* < .01

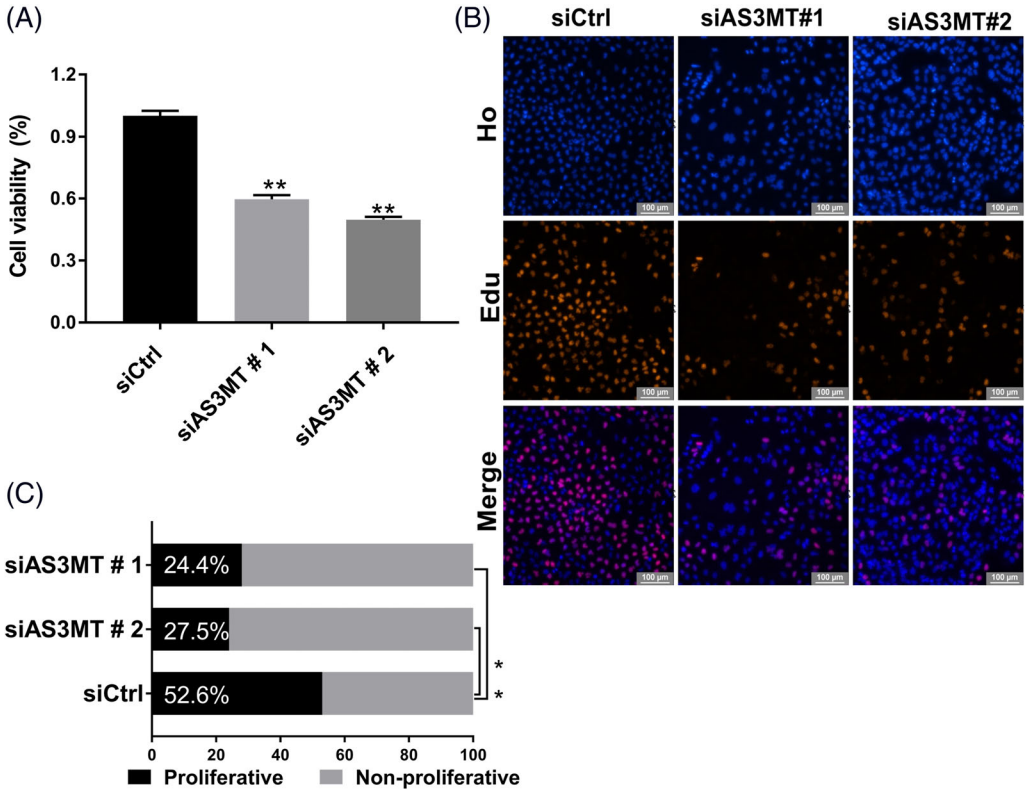

FIGURE 5 Knockdown of AS3MT significantly inhibited cell viability and proliferation. At 72 hours after transfection, A, the results of MTS assay revealed that the knockdown of AS3MT significantly inhibited cell viability (n = 4) (mean ± SEM, with Student's *t*-test). B, Cell proliferation assay revealed that the knockdown of AS3MT significantly inhibited cell proliferation, as assessed by fluorescence microscope. C, knockdown of AS3MT significantly inhibited efficiency of cell proliferation by imageJ software counting the number of cells in Figure 2B (percentage, with Chi-square test). **P* < .05, ***P* < .01 [Color figure can be viewed at wileyonlinelibrary.com]

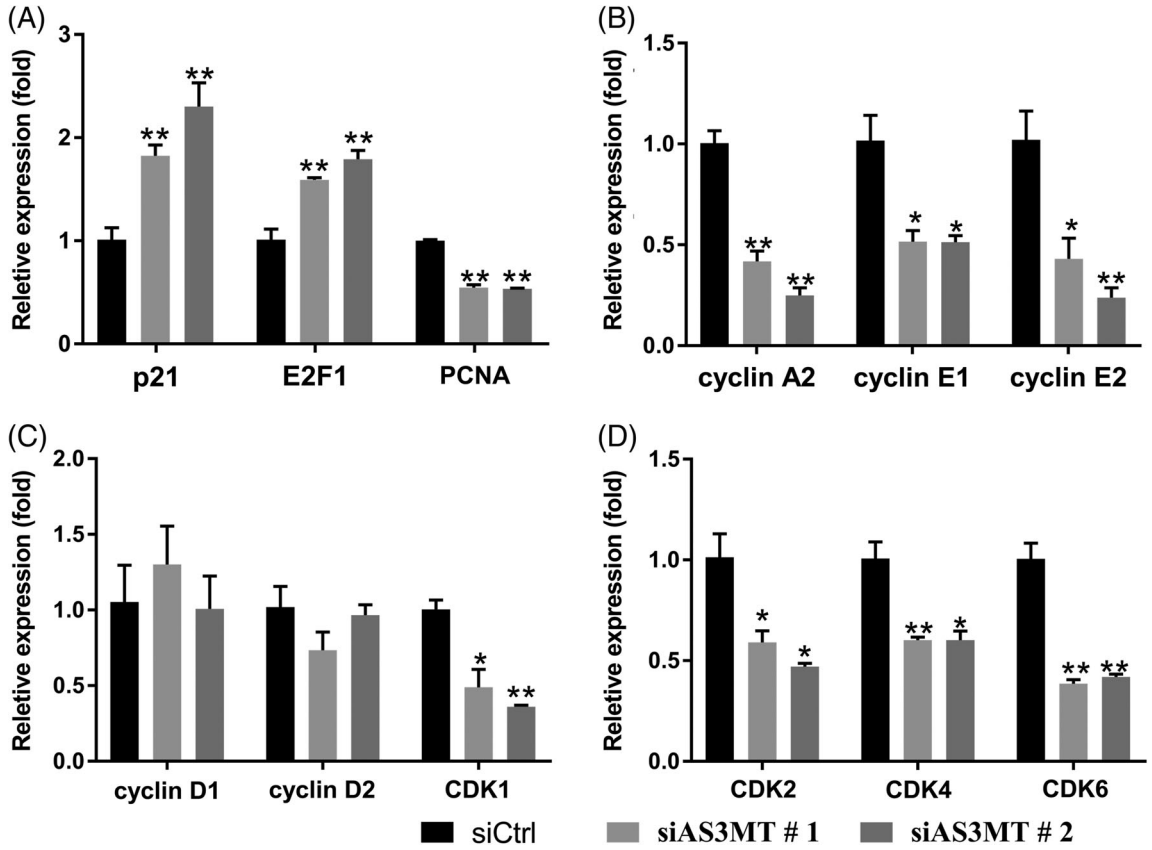

FIGURE 6 Knockdown of AS3MT regulated expression level of genes in A549 cell lines. At 72 hours after transfection, A, the qRT-PCR revealed that knockdown of AS3MT significantly increased expression of p21 and E2F1 mRNA, and inhibited expression levels of PCNA. B, Knockdown of AS3MT significantly inhibited the mRNA expression levels of cyclinA2, cyclinE1, and cyclinE2. C, There were no significant difference of the expression levels of CyclinD1 and CyclinD2 between siCtrl group and siAS3MT groups. D, Knockdown of AS3MT significantly inhibited expression levels of CDK1, CDK2, CDK4, and CDK6 mRNA (n = 3) (mean ± SEM, with Student's *t*-test). **P* < .05, ***P* < .01

qRT-PCR in A549 cells, such as cyclinE1, CDKs, and p21. During AS3MT down-expression, the expression levels of CDK1, CDK2, CDK4, CDK6, CyclinA2, CyclinE1, CyclinE2, and PCNA were inhibited in siAS3MT groups compared with siCtrl groups ($P < .05$) (Figure 6A-D). Compared with siCtrl groups, p21 and E2F1 expression were induced in siAS3MT groups ($P < .05$) (Figure 6A). However, There were no significant difference of the expression levels of CyclinD1 and CyclinD2 between siCtrl group and siAS3MT groups ($P > .05$) (Figure 6C).

4 | DISCUSSION

Occupational laborers were mainly exposed to trivalent inorganic arsenic from arsenic smelting plants. Metabolism of iAs in liver lead to formation MMA and DMA which eliminated by kidney into urine. DMA, MMA, and iAs in urine were defined as a biomarker of exogenous arsenic exposure.[21] However, the toxicity of MMA(III) was 26 times to that of iAs(III), and had a stronger ability to induced skin cancer, lung cancer, and bladder cancer.[22,23] Drobna Z study showed that the capacity to methylate iAs decreased by over 70% in human hepatocellular carcinoma with low AS3MT expression.[24] Additionally, previous studies have indicated that level of AS3MT mRNA was correlated with a large number of genes, such as p15 and TGF-beta.[16] Therefore, AS3MT could play an important role in arsenic carcinogenesis.

In this study, we evaluated the expression of AS3MT mRNA in populations exposed to arsenic by qRT-PCR. Our results indicated that AS3MT mRNA expression was increased in arsenic exposure group compared to control group. Furthermore, the result of Pearson correlation analysis showed that the level of AS3MT mRNA expression was positively correlated with the concentrations of urinary tAs, DMA, MMA, and iAs in all subjects. Subsequently, we wanted to know the expression of AS3MT in NSCLC tissues. Interestingly, the AS3MT expression was increased in human NSCLC tissues compared to their adjacent normal lung tissues. To our knowledge, this has not been reported in any studies. Generally speaking, AS3MT impact the risk of cancer by affecting arsenic metabolism.[11,13,14] But, it is unclear whether overexpression of AS3MT by arsenic exposure could directly act on the cell and affect the progression of NSCLC. Thus, it is necessary to explore functions and underlying mechanism of AS3MT in cancer.

To further confirm AS3MT expression with iAs exposure, we analyzed the expression of AS3MT in A549 cells with $NaAsO_2$ treatment. The data indicated that AS3MT mRNA expression was increased gradually in a concentration-dependent manner in A549 cells. This was

consistent with Eyvani's study in colorectal cancer cells.[25] Eyvani et al[25] stated that AS3MT had a crucial role in demethylation induced by As_2O_3. However, anomalous DNA methylation induced silencing of cell cycle genes and cell proliferation in different cancer.

Next, we want to explore whether AS3MT regulated proliferation of lung cancer cells. Our results indicated that knockdown of AS3MT significantly suppressed viability and proliferation of A549 cells. Aberrant cell proliferation is a characteristic of all cancer cells, and cell cycle regulatory genes are typically dysregulated in tumor cells.[26] For instance, Krüppel-like factors 16 (KLF16) regulated G0/G1 phase cell cycle transition by regulating p21 and CDK4, and promoted the proliferation of gastric cancer cells.[27] However, it remains unclear how AS3MT regulates the proliferation of A549 cells. Thus, we assessed the expression of 10 cell cycle regulatory genes in this research. Our data showed that knockdown of AS3MT inhibited proliferation by regulating several important cell cycle genes, including up-regulating p21 and E2F1 mRNA expression, and inhibiting mRNA expression levels of CDK1, CDK2, CDK4, CDK6, Cyclin A2, Cyclin E1, Cyclin E2, and PCNA. This result is consistent with that from Tian.[28] Our result revealed that knockdown of AS3MT inhibited cell proliferation.

Studies indicated that arsenic induced abnormal methyltransferase was often related to tumorigenesis.[29] However, iAs could also increase AS3MT expression and consume much SAM to methylate arsenic, which cause aberrant DNA methylation. Aberrant DNA methylation plays a major role for cell cycle, for instance, gene transcription level of p21 was regulated by DNA methylation.[30] P21, CDK-interacting protein 1, plays a critical role on the G1-S transition.[31] Studies reported that p21 reduced the activity of cyclin-CDK complexes,and inhibited DNA synthesis by binding to PCNA.[32,33] In addition, Phalke et al[34] reported that protein arginine methyltransferase 6 exhibited an oncogenic function by directly binding to and inhibiting the promoter of p21. Lu et al[35] found that the histone methyltransferase SETDB1 directly binds to the STAT1 promoter region and mediated colorectal cancer cell proliferation by STAT1-CCND1/CDK6 axis. Similarly, AS3MT may also exhibit an oncogenic function by directly binding to cell cycle genes.

In conclusion, our results demonstrated that inorganic arsenic increased AS3MT expression in vitro and in vivo. AS3MT, overexpression in NSCLC tissues, induced the proliferation of lung cancer cells by regulated p21, CDKs, Cyclin A2, Cyclin E1, Cyclin E2, PCNA, and E2F1. These results suggested that overexpression of AS3MT by arsenic exposure could directly act on the cell and affect the progression of NSCLC.

ACKNOWLEDGMENTS

This study was funded by a grant from the Nature Science Fund of China (81160343); The Yunnan Provincial Department of Education Science Research Fund Project (2019Y0259) and Ten Thousand Talent Program of Yunnan Province.

CONFLICT OF INTEREST

The authors declare that they have no known competing financial interests or personal relationships that could have appeared to influence the work reported in this article.

ORCID

Yuefeng He https://orcid.org/0000-0002-4604-8064

REFERENCES

1. Boffetta P, Borron C. Low-level exposure to arsenic in drinking water and risk of lung and bladder cancer: a systematic review and dose-response meta-analysis. *Dose Response*. 2019;17(3):711654830.
2. Wen W, Lu L, He Y, et al. LincRNAs and base modifications of p53 induced by arsenic methylation in workers. *Chem Biol Interact*. 2016; 246:1-10.
3. Chen QY, Li J, Sun H, et al. Role of miR-31 and SATB2 in arsenic-induced malignant BEAS-2B cell transformation. *Mol Carcinog*. 2018; 57(8):968-977.
4. Fang X, Sun R, Hu Y, et al. miRNA-182-5p, via HIF2α, contributes to arsenic carcinogenesis: evidence from human renal epithelial cells. *Metallomics*. 2018;10(11):1607-1617.
5. Martinez VD, Becker-Santos DD, Vucic EA, Lam S, Lam WL. Induction of human squamous cell-type carcinomas by arsenic. *J Skin Cancer*. 2011;2011:454157.
6. Wang Y, Shen Y, Sun X, Hong TL, Huang LS, Zhong M. Prognostic roles of the expression of sphingosine-1-phosphate metabolism enzymes in non-small cell lung cancer. *Transl Lung Cancer Res*. 2019; 8(5):674-681.
7. Kuo YC, Lo YS, Guo HR. Lung cancer associated with arsenic ingestion: cell-type specificity and dose response. *Epidemiology*. 2017; 28(Suppl 1):S106-S112.
8. He W, Zhang Y, Xia S. LncRNA NNT-AS1 promotes non-small cell lung cancer progression through regulating miR-22-3p/YAP1 axis. *Thorac Cancer*. 2020;11:549-560.
9. Gamboa-Loira B, Cebrian ME, Franco-Marina F, Lopez-Carrillo L. Arsenic metabolism and cancer risk: a meta-analysis. *Environ Res*. 2017;156:551-558.
10. Wei B, Yu J, Kong C, et al. Effects of arsenic methylation and metabolism on the changes of arsenic-related skin lesions. *Environ Sci Pollut Res Int*. 2018;25(24):24394-24402.
11. de la Rosa R, Steinmaus C, Akers NK, et al. Associations between arsenic (+3 oxidation state) methyltransferase (AS3MT) and N-6 adenine-specific DNA methyltransferase 1 (N6AMT1) polymorphisms, arsenic metabolism, and cancer risk in a chilean population. *Environ Mol Mutagen*. 2017;58(6):411-422.
12. Park S, Park JE, Yoo HJ, et al. Family-based association study of the arsenite methyltransferase gene (AS3MT, rs11191454) in Korean children with attention-deficit hyperactivity disorder. *Psychiatr Genet*. 2015;25(1):26-30.
13. Lin YC, Chen WJ, Huang CY, et al. Polymorphisms of arsenic (+3 oxidation state) Methyltransferase and arsenic methylation capacity affect the risk of bladder cancer. *Toxicol Sci*. 2018;164(1):328-338.
14. Huang CY, Lin YC, Shiue HS, et al. Comparison of arsenic methylation capacity and polymorphisms of arsenic methylation genes between bladder cancer and upper tract urothelial carcinoma. *Toxicol Lett*. 2018;295:64-73.
15. Du Y, Zhu J, Chu BF, Yang YP, Zhang SL. MiR-548c-3p suppressed the progression of papillary thyroid carcinoma via inhibition of the HIF1alpha-mediated VEGF signaling pathway. *Eur Rev Med Pharmacol Sci*. 2019;23(15):6570-6578.
16. Cheng H, Hu P, Wen W, Liu L. Relative miRNA and mRNA expression involved in arsenic methylation. *PLoS One*. 2018;13(12):e209014.
17. Korovaitseva GI, Gabaeva MV, Yunilainen OA, Golimbet VE. Effect of VNTR polymorphism of the AS3MT gene and Obstetrical complications on the severity of schizophrenia. *Bull Exp Biol Med*. 2019;168(1): 84-86.
18. Kang JU, Koo SH, Kwon KC, Park JW. AMY2A: a possible tumor-suppressor gene of 1p21.1 loss in gastric carcinoma. *Int J Oncol*. 2010;36(6):1429-1435.

19. He Y, Zhang R, Song X, Shang L, Wu X, Huang D. Inorganic arsenic exposure increased expression of Fas and Bax gene in vivo and vitro. *Gene*. 2018;671:135-141.
20. Sun G, Xu Y, Li X, Jin Y, Li B, Sun X. Urinary arsenic metabolites in children and adults exposed to arsenic in drinking water in Inner Mongolia, China. *Environ Health Perspect*. 2007;115(4):648-652.
21. Wei B, Yu J, Wang J, et al. The relationships between arsenic methylation and both skin lesions and hypertension caused by chronic exposure to arsenic in drinking water. *Environ Toxicol Pharmacol*. 2017;53:89-94.
22. Wei BG, Ye BX, Yu JP, et al. Blood pressure associated with arsenic methylation and arsenic metabolism caused by chronic exposure to arsenic in tube well water. *Biomed Environ Sci*. 2017;30(5):334-342.
23. Zhang Q, Li Y, Liu J, Wang D, Zheng Q, Sun G. Differences of urinary arsenic metabolites and methylation capacity between individuals with and without skin lesions in Inner Mongolia, northern China. *Int J Environ Res Public Health*. 2014;11(7):7319-7332.
24. Drobna Z, Xing W, Thomas DJ, Styblo M. shRNA silencing of AS3MT expression minimizes arsenic methylation capacity of HepG2 cells. *Chem Res Toxicol*. 2006;19(7):894-898.
25. Eyvani H, Moghaddaskho F, Kabuli M, et al. Arsenic trioxide induces cell cycle arrest and alters DNA methylation patterns of cell cycle regulatory genes in colorectal cancer cells. *Life Sci*. 2016;167:67-77.
26. Sherr CJ. Cancer cell cycles. *Science*. 1996;274(5293):1672-1677.
27. Ma P, Sun CQ, Wang YF, et al. KLF16 promotes proliferation in gastric cancer cells via regulating p21 and CDK4. *Am J Transl Res*. 2017;9(6):3027-3036.
28. Tian H, Zhang Y, Zhang Q, Li S, Liu Y, Han X. Effects of BENC-511, a novel PI3K inhibitor, on the proliferation and apoptosis of A549 human lung adenocarcinoma cells. *Biosci Trends*. 2019;13(1):40-48.
29. Yang SM, Huang CY, Shiue HS, et al. Combined effects of DNA methyltransferase 1 and 3A polymorphisms and urinary total arsenic levels on the risk for clear cell renal cell carcinoma. *Toxicol Appl Pharmacol*. 2016;305:103-110.
30. Lu Y, Qu H, Qi D, et al. OCT4 maintains self-renewal and reverses senescence in human hair follicle mesenchymal stem cells through the downregulation of p21 by DNA methyltransferases. *Stem Cell Res Ther*. 2019;10(1):28.
31. Liu JQ, Feng YH, Zeng S, Zhong MZ. linc01088 promotes cell proliferation by scaffolding EZH2 and repressing p21 in human non-small cell lung cancer. *Life Sci*. 2020;241:117134.
32. Kreis NN, Louwen F, Yuan J. Less understood issues: p21(Cip1) in mitosis and its therapeutic potential. *Oncogene*. 2015;34(14):1758-1767.
33. Waga S, Hannon GJ, Beach D, Stillman B. The p21 inhibitor of cyclin-dependent kinases controls DNA replication by interaction with PCNA. *Nature*. 1994;369(6481):574-578.
34. Phalke S, Mzoughi S, Bezzi M, et al. p53-independent regulation of p21Waf1/Cip1 expression and senescence by PRMT6. *Nucleic Acids Res*. 2012;40(19):9534-9542.
35. Lu Y, Feng Y, Yi-Yi L, et al. Histone methyltransferase SETDB1 promotes colorectal cancer proliferation through the STAT1-CCND1/CDK6 axis. *Carcinogenesis*. 2020;41(5):678-688.

How to cite this article: Sun M, Tan J, Wang M, Wen W, He Y. Inorganic arsenic-mediated upregulation of AS3MT promotes proliferation of nonsmall cell lung cancer cells by regulating cell cycle genes. *Environmental Toxicology*. 2020; 1–9. https://doi.org/10.1002/tox.23026